

## Structural Dynamics of the Cooperative Binding of Organic Molecules in the Human Cytochrome P450 3A4

Dan Fishelovitch,<sup>†</sup> Carina Hazan,<sup>‡</sup> Sason Shaik,<sup>‡</sup> Haim J. Wolfson,<sup>§</sup>  
and Ruth Nussinov<sup>\*,†,||</sup>

*Contribution from the Department of Human Genetics, Sackler Institute of Molecular Medicine, Sackler Faculty of Medicine, Tel Aviv University, Tel Aviv 69978, Institute of Chemistry and Lise-Meitner-Minerva Center for Computational Quantum Chemistry, The Hebrew University of Jerusalem, Jerusalem 91904, and School of Computer Science, Tel Aviv University, Tel Aviv 69978, Israel, and SAIC-Frederick, Inc., Center for Cancer Research Nanobiology Program, NCI-Frederick, Building 469, Room 151, Frederick, Maryland 21702*

Received August 18, 2006; E-mail: ruthn@ncifcrf.gov

**Abstract:** Cytochrome P450 3A4 (CYP3A4) is a key enzyme responsible for the metabolism of 50% of all orally administered drugs which exhibit an intriguing kinetic behavior typified by a sigmoidal dependence of the reaction velocity on the substrate concentration. There is evidence for the binding of two substrates in the active site of the enzyme, but the mechanism of this cooperative binding is unclear. Diazepam is such a drug that undergoes metabolism by CYP3A4 with sigmoidal dependence. Metabolism is initiated by hydrogen atom abstraction from the drug. To understand the factors that determine the cooperative binding and the juxtaposition of the C–H bond undergoing abstraction, we carried out molecular dynamics simulations for two enzymatic conformers and examined the differences between the substrate-free and the bound enzymes, with one and two diazepam molecules. Our results indicate that the effector substrate interacts both with the active substrate and with the enzyme, and that this interaction results in side chain reorientation with relatively minor long-range effects. In accord with experiment, we find that F304, in the interface between the active and effector binding sites, is a key residue in the mechanism of cooperative binding. The addition of the effector substrate stabilizes F304 and its environment, especially F213, and induces a favorable orientation of the active substrate, leading to a short distance between the targeted hydrogen for abstraction and the active species of the enzyme. In addition, in one conformer of the enzyme, residue R212 may strongly interact with F304 and counteract the effector's impact on the enzyme.

### 1. Introduction

Cytochrome P450 3A4 (CYP3A4) is a human enzyme that belongs to a superfamily (denoted P450) of heme-containing enzymes that function as monooxygenases of a variety of chemical compounds in microorganisms, plants, and mammals.<sup>1</sup> For a given substrate, P450 enzymes can catalyze a wide variety of reactions, such as hydroxylation, epoxidation or heteroatom oxidation, dealkylations, and desaturation.<sup>2</sup> The human CYP3A4 isoform oxidizes about 50% of all drugs taken orally<sup>3</sup> and is therefore of high interest to the pharmaceutical industry and in medicinal chemistry. The oxidation reaction occurs at the hydrophobic core of the protein where the active species of the

enzyme activates a bond in the substrate by hydrogen abstraction and thereby leads to its oxidation.

The majority of the monooxidation reactions in P450 enzymes involve the active species called “compound I” (CpdI), which is a ferryl–porphyrin– $\pi$  cation radical created during the catalytic cycle after consumption of two protons and electrons followed by a heterolytic cleavage of molecular oxygen.<sup>4</sup> CYP3A4 has a large active site and can oxidize many substrates with diverse chemical structures. Several P450's including the 3A4 isoform exhibit an atypical steady-state kinetics in vitro and presumably in vivo as judged by the sigmoidal reaction velocity vs substrate concentration plots. CYP3A4 manifests atypical kinetics with several substrates and drugs including testosterone,<sup>5,6</sup> estradiol,<sup>6</sup> progesterone,<sup>7</sup> amitriptyline,<sup>8</sup> diazepam,<sup>9</sup> carbamazepine,<sup>10</sup> aflatoxinB1,<sup>11</sup> midazolam,<sup>12</sup> and  $\alpha$ -naph-

<sup>†</sup> Sackler Faculty of Medicine, Tel Aviv University.

<sup>‡</sup> The Hebrew University of Jerusalem.

<sup>§</sup> School of Computer Science, Tel Aviv University.

<sup>||</sup> NCI-Frederick.

- (1) Guengerich F. P. In *Cytochrome P450: Structure, Mechanism and Biochemistry*, 3rd ed.; Ortiz de Montellano, P. R., Ed.; Plenum Press: New York, 2005; pp 377–531.
- (2) Guengerich, F. P. *Chem. Res. Toxicol.* **2001**, *14*, 611–650.
- (3) Wrighton, S. A.; Schuetz, E. G.; Thummel, K. E.; Shen, D. D.; Korzekwa, K. R.; Watkins, P. B. *Drug Metab. Rev.* **2000**, *32*, 339–361.
- (4) Meunier, B.; de Visser, S. P.; Shaik, S. *Chem. Rev.* **2004**, *104*, 3947–3980.
- (5) Harlow, G. R.; Halpert, J. R. *Proc. Natl. Acad. Sci. U.S.A.* **1998**, *95*, 6636–6641.

- (6) Ueng, Y. F.; Kuwabara, T.; Chun, Y. J.; Guengerich, F. P. *Biochemistry* **1997**, *36*, 370–381.
- (7) Schwab, G. E.; Raucy, J. L.; Johnson, E. F. *Mol. Pharmacol.* **1988**, *33*, 493–499.
- (8) Schmider, J.; Greenblatt, D. J.; von Moltke, L. L.; Harmatz, J. S.; Shader, R. I. *J. Pharmacol. Exp. Ther.* **1995**, *275*, 592–597.
- (9) Andersson, T.; Miners, J. O.; Veronese, M. E.; Birkett, D. J. *Br. J. Clin. Pharmacol.* **1994**, *38*, 131–137.
- (10) Kerr, B. M.; Thummel, K. E.; Wurden, C. J.; Klein, S. M.; Kroetz, D. L.; Gonzalez, F. J.; Levy, R. H. *Biochem. Pharmacol.* **1994**, *47*, 1969–1979.

thoflavone.<sup>13</sup> Atypical kinetics, like allostery, requires the cooperative binding (CB) of two substrates to form a ternary complex between a P450 enzyme and the substrates. The substrate that binds inside the active site of the enzyme and undergoes oxidation is called the *active substrate*. The substrate that controls the active substrate oxidation is called the *effector substrate*. If both the active and effector substrates are identical, CB is referred to as homotropic cooperativity, otherwise as heterotropic cooperativity. A well-documented heterotropic cooperativity in CYP3A4 is the stimulation of  $\alpha$ -naphthoflavone on testosterone and progesterone hydroxylation.<sup>14</sup> According to the latest review on non-Michaelis–Menten kinetics in P450's,<sup>15</sup> not much is known about the mechanism of CB, but it has been proposed that it is related to the ability of CYP3A4 to accommodate multiple substrates within its active site.<sup>16–18</sup> One explanation for the atypical kinetics mechanism has been a ligand-dependent conformational change whereby each complex between the enzyme and a ligand adopts a different conformation of the P450 with a distinct kinetic profile.<sup>19–21</sup> A mechanistic proposition for CB suggests a direct effect of the effector substrate on the active one. The effector substrate may stabilize the active substrate inside the active site and enhance a favorable orientation of the active substrate for oxidation. Spectroscopic evidence in the case of pyrene<sup>22</sup> and theoretical predictions in the case of carbamazepine<sup>23</sup> strongly suggest the existence of two substrates stabilized by hydrogen bonds and  $\pi$ – $\pi$  interactions, within the same active site. Structural evidence for the existence of two substrates in the active site of a P450 comes from two X-ray structures of a bacterial CYPeryF<sup>24</sup> in which there are two identical substrates in the core of the protein at the active site. The phenomenon of CB in P450 enzymes differs from known allosteric regulation, in the sense that in allosteric proteins the effector site is usually distinct from the active site. In P450 enzymes not only can the active and effector sites be close, but also the cooperativity can be diverse: some effectors have a positive effect on the oxidation of the active substrate, and some have a negative effect. Yet the issue of cooperativity is still under debate with two possible binding sites of the effector: one in proximity to the binding site of the active substrate and the other in a remote site that resembles an allosteric site. Recently, using time-resolved fluorescence, Atkins et al.<sup>25</sup> have shown that testosterone exerts a heterotropic effect

on a fluorescent ligand in the active site, and this effect originates in the testosterone binding to a distinct binding site, distant from the heme moiety.<sup>25</sup> Nevertheless, the authors conclude that the effector binding site of testosterone can be a remote corner either *inside the active site* or at a distinct peripheral site. Clearly, a deeper mechanistic understanding of CB could improve predictions for drug–drug interactions and drug clearance and provide insights into a new type of allostery. This is a fundamental question of both mechanistic and pharmaceutical importance.

The present work studies the mechanism of CB in the CYP3A4 isoform by means of molecular dynamics (MD) simulations. To date, there are two unbound X-ray structures of CYP3A4<sup>26,27</sup> that are deposited in the PDB,<sup>28</sup> two structures with substrates, one bound outside the active site<sup>27</sup> and one inside the active site but without an oxidative binding mode,<sup>29</sup> and two structures with inhibitors coordinated to the heme moiety inside the active site.<sup>27,29</sup> The main difference between the two unbound structures is in the orientation of R212, which in one structure (PDB code 1W0E) is facing out of the active site and in the other (PDB code 1TQN) toward the heme group in the active site. The main difference between the two structures that include inhibitors is that in the first structure there is one inhibitor while in the second and more recently published structure<sup>29</sup> there are two ketoconazole molecules inside the active site. This doubly ligated structure illustrates that CYP3A4 can bind simultaneously multiple ligands.

Our study simulates three species of the enzyme: the unbound enzyme, the enzyme in complex with a drug, diazepam, known to undergo homotropic cooperativity,<sup>9,18,30</sup> and the enzyme with two diazepam molecules. Diazepam was docked following biological data which include single-site mutations that affected the drug binding to the enzyme and an alignment with the two CYPeryF structures having two substrates at the active site. Support for CB of diazepam inside the active site comes from an NMR T1 paramagnetic relaxation study<sup>12</sup> in which midazolam, a similar drug that shares the same benzodiazepine scaffold, undergoes CB with both active and effector substrates nested within the active site. For each of the three enzyme species, the simulations were carried out on the two unbound conformer structures of CYP3A4. The topology and parameter files for CpdI were taken from previous quantum mechanics/molecular mechanics (QM/MM) calculations (see section 2.1), and a new diazepam force field was developed here. We focused on the changes between structures bound to one or two substrates, by following the changes that the effector molecule exerts on the active one and by examining whether the different conformers exhibit different CB dynamic properties. We hope that the detailed structural dynamics performed here will provide clues to the mechanism of the homotropic cooperativity or CB

- (11) Xue, L.; Wang, H. F.; Wang, Q.; Szklarczyk, G. D.; Domanski, T. L.; Halpert, J. R.; Correia, M. A. *Chem. Res. Toxicol.* **2001**, *14*, 483–491.
- (12) Cameron, M. D.; Wen, B.; Allen, K. E.; Roberts, A. G.; Schuman, J. T.; Campbell, A. P.; Kunze, K. L.; Nelson, S. D. *Biochemistry* **2005**, *44*, 14143–14151.
- (13) Domanski, T. L.; He, Y. A.; Khan, K. K.; Roussel, F.; Wang, Q.; Halpert, J. R. *Biochemistry* **2001**, *40*, 10150–10160.
- (14) Domanski, T. L.; Liu, J.; Harlow, G. R.; Halpert, J. R. *Arch. Biochem. Biophys.* **1998**, *350*, 223–232.
- (15) Atkins, W. M. *Annu. Rev. Pharmacol. Toxicol.* **2005**, *45*, 291–310.
- (16) Shou, M.; Grogan, J.; Mancewicz, J. A.; Krausz, K. W.; Gonzalez, F. J.; Gelboin, H. V.; Korzekwa, K. R. *Biochemistry* **1994**, *33*, 6450–6455.
- (17) Korzekwa, K. R.; Krishnamachary, N.; Shou, M.; Ogai, A.; Parise, R. A.; Rettie, A. E.; Gonzalez, F. J.; Tracy, T. S. *Biochemistry* **1998**, *37*, 4137–4147.
- (18) He, Y. A.; Roussel, F.; Halpert, J. R. *Arch. Biochem. Biophys.* **2003**, *409*, 92–101.
- (19) Koley, A. P.; Buters, J. T.; Robinson, R. C.; Markowitz, A.; Friedman, F. K. *J. Biol. Chem.* **1997**, *272*, 3149–3152.
- (20) Atkins, W. M.; Wang, R. W.; Lu, A. Y. *Chem. Res. Toxicol.* **2001**, *14*, 338–347.
- (21) Koley, A. P.; Robinson, R. C.; Markowitz, A.; Friedman, F. K. *Biochem. Pharmacol.* **1997**, *53*, 455–460.
- (22) Dabrowski, M. J.; Schrag, M. L.; Wienkers, L. C.; Atkins, W. M. *J. Am. Chem. Soc.* **2002**, *124*, 11866–11867.
- (23) Torimoto, N.; Ishii, I.; Hata, M.; Nakamura, H.; Imada, H.; Ariyoshi, N.; Ohmori, S.; Igarashi, T.; Kitada, M. *Biochemistry* **2003**, *42*, 15068–15077.

- (24) Cupp-Vickery, J.; Anderson, R.; Hatziris, Z. *Proc. Natl. Acad. Sci. U.S.A.* **2000**, *97*, 3050–3055.
- (25) Lampe, J. N.; Atkins, W. M. *Biochemistry* **2006**, *45*, 12204–12215.
- (26) Yano, J. K.; Wester, M. R.; Schoch, G. A.; Griffin, K. J.; Stout, C. D.; Johnson, E. F. *J. Biol. Chem.* **2004**, *279*, 38091–38094.
- (27) Williams, P. A.; Cosme, J.; Vinkovic, D. M.; Ward, A.; Angove, H. C.; Day, P. J.; Vornrhein, C.; Tickle, I. J.; Jhoti, H. *Science* **2004**, *305*, 683–686.
- (28) Bernstein, F. C.; Koetzle, T. F.; Williams, G. J.; Meyer, E. F., Jr.; Brice, M. D.; Rodgers, J. R.; Kennard, O.; Shimanouchi, T.; Tasumi, M. *Eur. J. Biochem.* **1977**, *80*, 319–324.
- (29) Ekroos, M.; Sjögren, T. *Proc. Natl. Acad. Sci. U.S.A.* **2006**, *103*, 13682–13687.
- (30) Shou, M.; Mei, Q.; Ettore, M. W., Jr.; Dai, R.; Baillie, T. A.; Rushmore, T. H. *Biochem. J.* **1999**, *340*, 845–853.

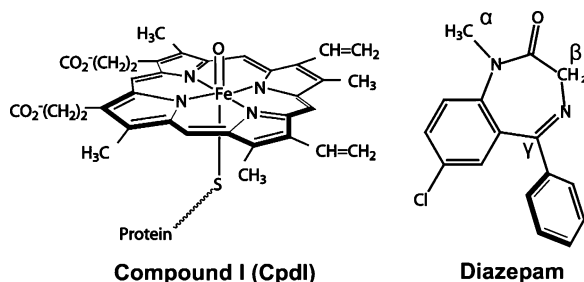


**Figure 1.** Chemical structures of the active oxygen species of CYP3A4 and CpdI and of the substrate diazepam.

of the CYP3A4 enzyme and will assist the prediction of drug metabolism and drug–drug interactions.

## 2. Computational Methods

**2.1. Protein Preparation.** The CYP3A4 structures were taken from the PDB<sup>28</sup> (codes 1TQN and 1W0E). Missing loop residues (282–285) of the 1TQN structure were modeled with InsightII (<http://www.accelrys.com/products/>). The missing residues of 1W0E were modeled by the Swiss-Pdb viewer<sup>31</sup> with the 1TQN structure as a template. The missing N terminus that is anchored to the ER membrane and the missing C terminus were not modeled since CYP3A4 manifests atypical kinetic curves in the membrane as well as in aqueous solutions.<sup>32</sup> For each CYP3A4 structure the  $pK_a$  values were calculated with the MCCE<sup>33</sup> software using Delphi<sup>34</sup> as a Poisson–Boltzmann solver with a dielectric constant of 4. Hydrogen atoms were added to the CYP3A4 structures with the HBUILD procedure of the CHARMM<sup>35</sup> software according to the calculated  $pK_a$  values, to give a total charge of +3. The coordinates of CpdI (Figure 1) were obtained from a structural alignment using the InsightII software according to atom selection between the CYP3A4 structures and a bacterial CYPcam structure (PDB code 1DZ9).<sup>36</sup> The proteins were solvated in a box containing ~21000 explicit TIP3P<sup>37</sup> water molecules. All the systems were neutralized by random placing of three chloride ions inside the water box. The force field of the CpdI heme active species was obtained from previous QM/MM calculations on CpdI by Schöneboom et al.<sup>38</sup> Parameters related to the active oxygen were taken from the added parameters of Bathelt et al.<sup>39</sup>

**2.2. Substrate Parametrization.** The CYP3A4 substrate chosen for the molecular dynamics study was diazepam (Figure 1). Diazepam coordinates were taken from the Cambridge Structural Database (<http://www.ccdc.cam.ac.uk/products/csd/>, code DIZPAM10), and the structure was further optimized at the B3LYP/6-31G\* level of theory followed by a frequency calculation. All QM calculations were performed using Gaussian98.<sup>40</sup> ESP charges were then calculated, and force constants were adjusted to the CHARMM27<sup>41</sup> force field and scaled to compensate for the harmonic approximation to the potential energy surface (<http://srdata.nist.gov/cccbdb/vsf.asp>, National Institute of Standards and

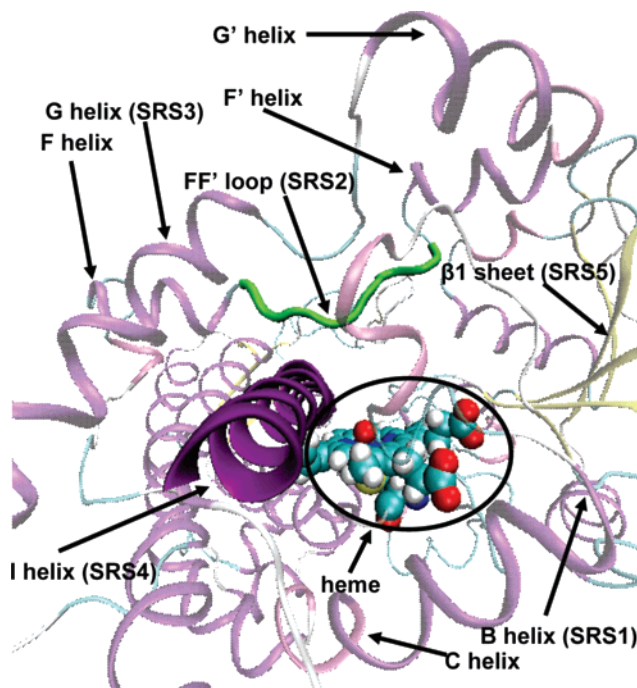


**Figure 2.** Overall fold of CYP3A4 colored according to secondary structures. Highlighted are the conserved I helix (purple) and the FF' loop (green). The heme group inside the core of the enzyme active site is represented using VDW spheres.

Technology<sup>42</sup>). Full parametrization procedures and representation of the diazepam force field are provided in the Supporting Information (SI).

**2.3. Docking Procedure.** To address the flexibility of the substrate, a conformational search for diazepam was performed using the Cerius2 (<http://www.accelrys.com/products/>) software. We used a systematic search algorithm which accounts for dihedral angles. Since the only rotatable dihedral angle is between the benzyl moiety and the  $\gamma$  carbon (Figure 1), this dihedral angle was rotated with a 15° step. Each diazepam conformer was docked into the enzyme using the PatchDock<sup>43</sup> software. The docking simulation of CB for diazepam was based on previous experimental work involving point mutations that led to the hindrance of the diazepam binding to CYP3A4<sup>18</sup> and on a structural alignment of CYP3A4 with the bacterial CYPeryF structures (PDB codes 1EUP and 1EGY) containing two identical substrates in the active site of the enzyme. Residues in CYP3A4 that correspond to those within 5 Å of the CYPeryF substrates were derived from the structural alignment performed by MultiProt.<sup>44</sup> The key binding residues found from the structural alignment combined with the mutational studies formed a biological scoring function for the diazepam docking to CYP3A4. The active diazepam was docked into the enzyme in a favorable orientation for hydroxylation of the  $\beta$  carbon hydrogens (Figure 1). Docking solutions with a distance of less than 2 Å between the  $\beta$  carbon hydrogens and the active oxygen were accepted. Of the resulting solutions, the complex with the lowest energy was chosen (MD energy in CHARMM27). For complexes with two substrates, a second diazepam molecule was docked into this model, and the lowest energy complex was chosen here too.

**2.4. System MD Simulations.** The following procedure was applied to all MD simulations: The force field used for all the simulations was CHARMM27 with the protein nucleic acid topology and parameter

(31) Guex, N.; Peitsch, M. C. *Electrophoresis* **1997**, *18*, 2714–2723.

(32) Schrag, M. L.; Wienkers, L. C. *Drug Metab. Dispos.* **2000**, *28*, 1198–1201.

(33) Georgescu, R. E.; Alexov, E. G.; Gunner, M. R. *Biophys. J.* **2002**, *83*, 1731–1748.

(34) Rocchia, W.; Alexov, E.; Honig, B. *J. Phys. Chem. B* **2001**, *105*, 6507–6514.

(35) Brooks, B. R.; Bruccoleri, R. E.; Olafson, B. D.; States, D. J.; Swaminathan, S.; Karplus, M. *J. Comput. Chem.* **1983**, *4*, 187–217.

(36) Schlichting, I.; Berendzen, J.; Chu, K.; Stock, A. M.; Maves, S. A.; Benson, D. E.; Sweet, R. M.; Ringe, D.; Petsko, G. A.; Sligar, S. G. *Science* **2000**, *287*, 1615–1622.

(37) Jorgensen, W. L.; Chandrasekhar, J.; Madura, J. D.; Impey, R. W.; Klein, M. L. *J. Chem. Phys.* **1983**, *79*, 926–935.

(38) Schöneboom, J. C.; Lin, H.; Reuter, N.; Thiel, W.; Cohen, S.; Ogliaro, F.; Shaik, S. *J. Am. Chem. Soc.* **2002**, *124*, 8142–8151.

(39) Bathelt, C. M.; Zurek, J.; Mulholland, A. J.; Harvey, J. N. *J. Am. Chem. Soc.* **2005**, *127*, 12900–12908.

(40) Frisch, M. J.; et al. *Gaussian 98*, revision A.11.2; Gaussian, Inc.: Pittsburgh, PA, 2001.

(41) MacKerell, A. D., Jr.; et al. *J. Phys. Chem. B* **1998**, *102*, 3586–3616.

(42) Scott, A. P.; Radom, L. *J. Phys. Chem.* **1996**, *100*, 16502–16513.

(43) Duhovny, D.; Nussinov, R.; Wolfson, H. J. *2nd Workshop on Algorithms in Bioinformatics (WABI'02), Rome, Italy, 2002*; Lecture Notes in Computer Science 2452; Springer: New York, 2002; pp 185–200.

(44) Shatsky, M.; Nussinov, R.; Wolfson, H. J. *Proteins* **2004**, *56*, 143–156.

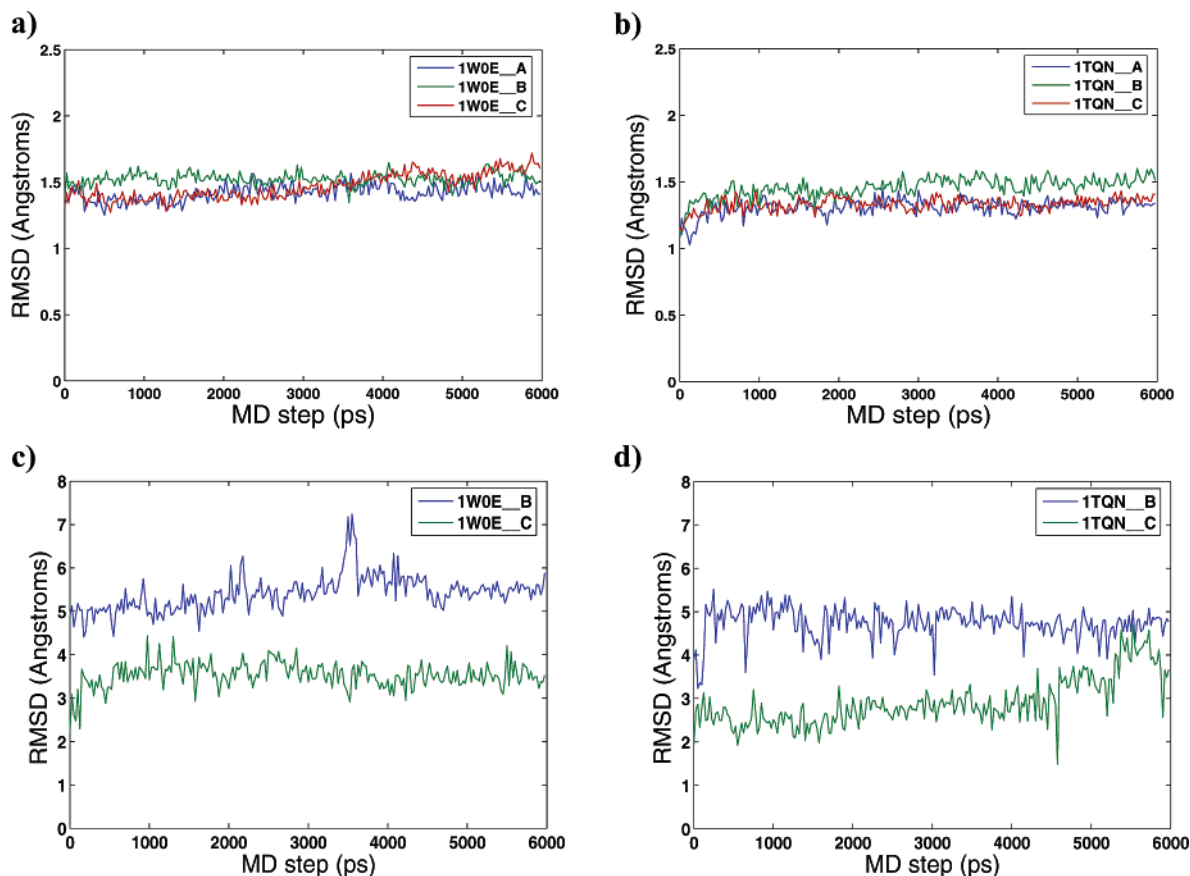


**Figure 3.** (a) C $\alpha$  RMSD between the frames along the simulation trajectory and the initial structure in the 1W0E conformer simulations. (b) C $\alpha$  RMSD between the frames along the trajectory and the initial structure in the 1TQN conformer simulations. (c) Total atom RMSD from the initial structure of the active diazepam as a function of time along the MD simulations with active diazepam docked to the 1W0E bound to one substrate (1W0E\_B) and to two substrates (1W0E\_C). (d) Total atom RMSD from the initial structure of the active diazepam as a function of time along the MD simulations with active diazepam docked to the 1TQN bound to one substrate (1TQN\_B) and to two substrates (1TQN\_C).

files. The systems were minimized by the CHARMM software with a decreasing harmonic force constraint on the enzyme with a tolerance gradient of 10 kcal/mol. The MD protocol of the minimized system included full minimization, heating, equilibration, and production all done with NAMD version 2.6b1 software.<sup>45</sup> The system was minimized for 300 steps using the steepest descent algorithm, then gradually heated to 310 K, and equilibrated for 50000 steps. All simulations were carried out for 6 ns, using a canonical NVT ensemble with periodic boundary conditions and with a time step of 1 fs. The twin bound conformers were simulated for an additional 6 ns to a total of 12 ns. The temperature was kept at 310 K. The ShakeH algorithm was applied to fix all bond lengths involving hydrogen atoms. We used a final nonbonded interaction cutoff radius of 12 Å with a smoothing cutoff of 10 Å. Full nonbonded electrostatic interactions were calculated with the particle mesh EWALD summation.<sup>46</sup> Trajectories were sampled every 0.25 ps.

### 3. Results and Discussion

**3.1 RMSD Analysis.** Three MD simulations were performed with the 1TQN CYP3A4 conformer in the following states: the unbound state and the bound states complexed with one and with two diazepam molecules. These states are denoted as 1TQN\_A, 1TQN\_B, and 1TQN\_C, respectively. Similar MD simulations were carried out on the 1W0E CYP3A4 conformer and are denoted 1W0E\_A, 1W0E\_B, and 1W0E\_C. There are two main metabolism pathways for diazepam: one involves

N-demethylation of carbon  $\alpha$ , forming nordiazepam (NDZ), and the other hydroxylation of carbon  $\beta$ , forming temazepam (TMZ) (Figure 1). The kinetics of formation of both metabolites is atypical, but the degree of sigmoidicity was observed to be greater for hydroxylation than for N-demethylation. In addition, the ratio of NDZ to TMZ formation increased as the diazepam concentration decreased.<sup>9</sup> CB of the hydroxylation reaction was simulated by docking the active diazepam in a favorable configuration for hydroxylation with the  $\beta$  carbon hydrogen atoms facing the active oxygen and adding the effector diazepam above the active one (see the Computational Methods). The P450 superfamily has a single conserved fold in SCOP<sup>47</sup> with only minor fold species variation, suggesting that the fold is energetically stable and no significant total RMSD fluctuations may be expected to occur. Figure 2 presents the enzyme fold. The total C $\alpha$  RMSD from the initial structures along the trajectory for all simulations did not change much and was equilibrated after  $\sim$ 1 ns of simulation, even in the presence of one or two substrates within the active site (Figure 3a,b). The final total C $\alpha$  RMSD from the initial structures is no more than 1.7 Å. The overall C $\alpha$  RMSD between the two ketoconazoles bound and erythromycin bound to CYP3A4 structures<sup>29</sup> and the ligand-free structure is fairly low according to MultiProt<sup>44</sup> ( $\sim$ 1 Å), but a substantial local movement occurs in the region of the FG helices which is suspected to be an effector binding site.

(45) Kale, L.; Skeel, R.; Bhandarkar, M.; Brunner, R.; Gursoy, A.; Krawetz, N.; Phillips, J.; Shinozaki, A.; Varadarajan, K.; Schulten, K. *J. Comput. Phys.* **1999**, *151*, 283–312.

(46) Petersen, H. G. *J. Chem. Phys.* **1995**, *103*, 3668–3679.

(47) Murzin, A. G.; Brenner, S. E.; Hubbard, T.; Chothia, C. *J. Mol. Biol.* **1995**, *247*, 536–540.

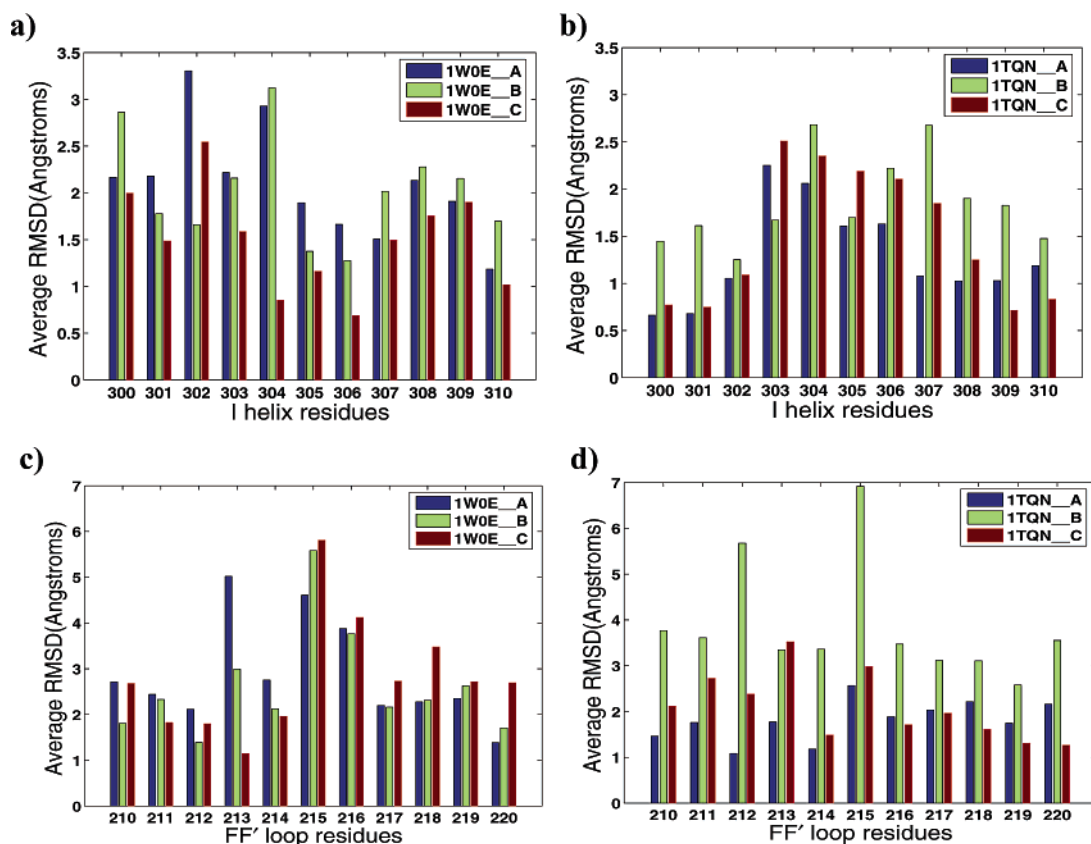


**Figure 4.** Average all-atom RMSD from the initial structures of the I helix and FF' residues in the six simulations: (a) I helix residues in the 1W0E conformer; (b) I helix residues in the 1TQN conformer; (c) FF' loop residues in the 1W0E conformer; (d) FF' loop residues in the 1TQN conformer.

However, since most CYP3A4 substrates that undergo CB are fairly small compared with ligands such as erythromycin or ketoconazole, with no more than four rigid rings and three rotatable dihedral angles, it is expected that the binding of these molecules will not cause as large of movements as those reported for erythromycin or ketoconazole. We believe that, due to the versatile spectrum of substrates with different sizes, shapes, and degrees of freedom, CYP3A4 can adopt different modes of binding. The overall atom RMSD from the initial structures vs time of active diazepam docked to the CYP3A4 conformers is shown in Figure 3c,d. Addition of the effector diazepam initially lowered the RMSD of the active diazepam in both conformers; however, in the 1TQN conformer it increased, and after 6 ns the active diazepam RMSD between 1TQN\_C and 1TQN\_B was only 1 Å. The active diazepam RMSD between 1W0E\_C and 1W0E\_B simulations after 6 ns was around 3 Å, so the impact of the effector on the active diazepam was larger in the 1W0E conformer. We calculated the C $\alpha$  RMSD of a multiple structural alignment between all CYPeryF structures in the PDB, including structures with two substrates within the active site, structures with only one substrate, and structures with an inhibitor. The total calculated C $\alpha$  RMSD of the alignment was 0.52 Å. Coupled with the fact that the total RMSD in all six simulations did not change much and was not influenced by the docked diazepam molecules, this suggests that, once inside the enzyme, the active and effector substrates have little effect on the global conformation of the protein. The 1W0E\_C and 1TQN\_C 12 ns simulations confirmed the convergence of our simulations with average C $\alpha$  enzyme RMSD's of 1.5 and 1.38 Å from the respective initial

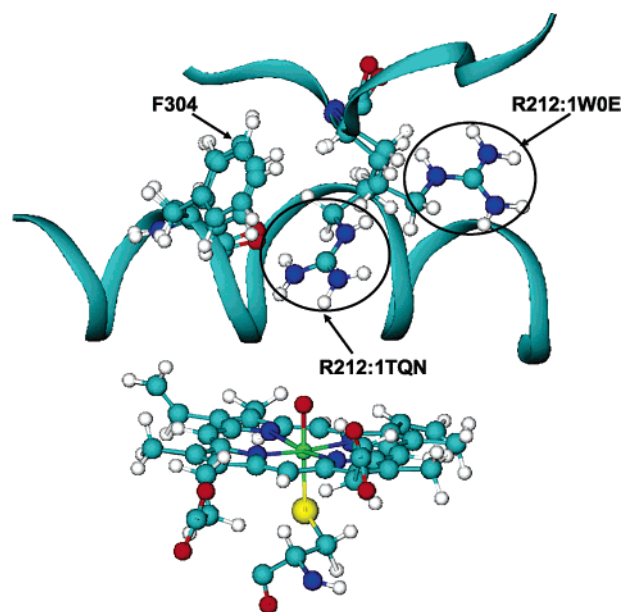


**Figure 5.** Pairwise structural alignment between the 1TQN and 1W0E PDB files. The I helix and the FF' loop are represented as ribbons and the heme moiety, C442, F304, and R212 as CPK models.

structures. There was no substantial change in the active diazepam RMSD in either of the conformers, and the final all-atom RMSD's obtained were 3.3 and 4.8 Å in the 1W0E\_C and 1TQN\_C simulations, respectively, from the initial structures (see the SI).

It was observed that, in the two structures of CYPeryF that exhibit homotropic cooperativity, a conserved A305 located in

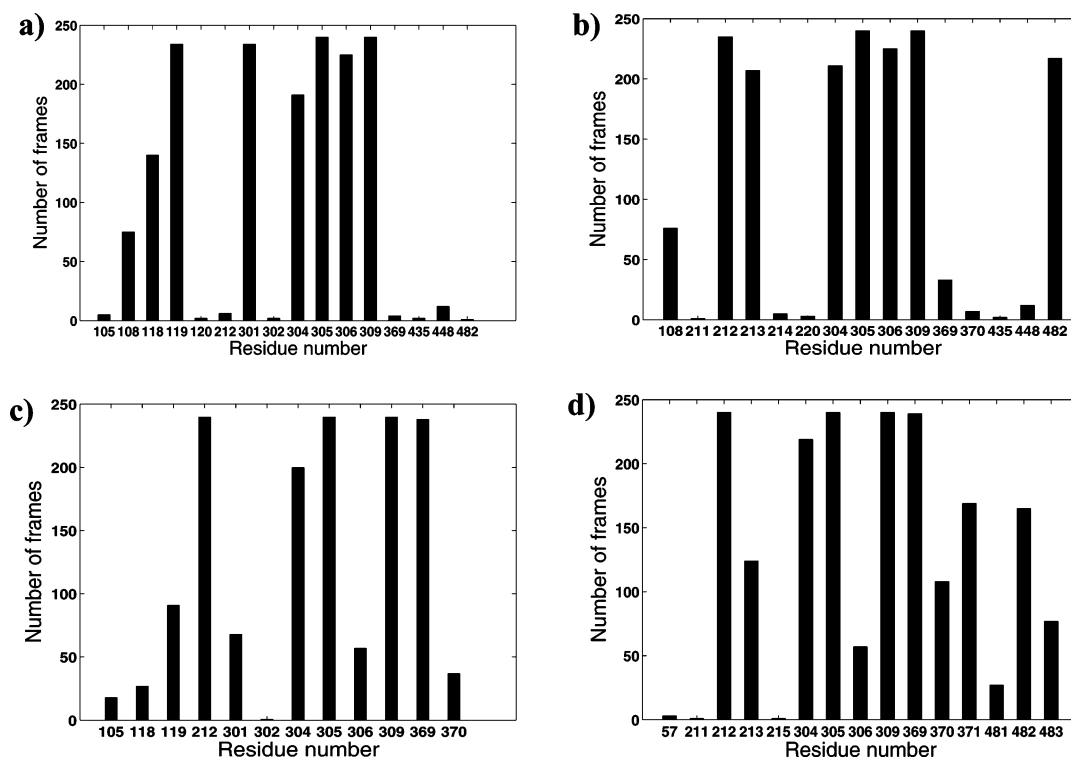


**Figure 6.** Number of frames over the simulation that contain a contact of less than 5 Å between each CYP3A4 residue and a diazepam molecule: (a) contacts between the active diazepam and the 1W0E conformer; (b) contacts between the effector diazepam and the 1W0E conformer; (c) contacts between the active diazepam and the 1TQN conformer; (d) contacts between the effector diazepam and the 1TQN conformer.

the I helix close to the heme moiety is in close contact with both the active and effector substrates.<sup>24</sup> This structural observation led us to suspect that residues in the vicinity of the conserved A305 are part of the interface between the active and effector sites and may play a role in the mechanism of CB. These residues include the conserved I helix residues that are connected to A305 and are proximal to the heme moiety and the flexible FF' loop, which caps the active site and connects helices F and F'. Figure 4 shows the calculated average *all-atom* RMSD of the I helix and FF' residues in the 6 ns simulations. The major effect of the addition of the effector diazepam molecule on the 1W0E conformer is a dramatic decrease of the RMSD of F304 from ~3.5 Å to less than 1 Å (Figure 4a) and to further decrease the RMSD of F213 to ~1 Å (Figure 4c). Addition of the effector diazepam did not change much the RMSD of F304 and F213 in the 1TQN conformer (Figure 4b,d). The impact of the effector diazepam on the 1TQN conformer is to decrease the RMSD of F215 and R212 of the FF' loop (Figure 4d). In the unbound conformation, the F304 residue is much more flexible in the 1W0E conformer than in the 1TQN conformer (Figure 4a,b). This can be explained by the strong interaction between R212 and F304 in the 1TQN conformer, where R212 faces from the top of the active site toward F304 (Figure 5). In the 1W0E conformer, R212 forms a salt bridge with E308 and faces outside the active site. Despite its suspected flexibility, in both conformers the orientation of R212 did not change much throughout the entire simulations due to the fact that the interactions are mainly electrostatic and the orientation is a local minimum. The intimate interactions between F304 and R212 in the 1TQN conformer prevent the effector from strongly interacting with F304 and explain the different effects of the effector substrate on each conformer.

**3.2. Close Contact Analysis.** It was previously shown that although there is low sequence identity between members of the P450 family, all have six distinct structural regions called substrate recognition sites (SRSs), which bind substrates.<sup>48,49</sup> The fold contains 12 helices denoted A–L and 5  $\beta$  sheets denoted 1–5.<sup>50</sup> To characterize the active and effector binding site residues, contacts of less than 5 Å between the diazepam molecules and the CYP3A4 conformers were measured along the MD trajectories (Figure 6). In addition, the structures of two conformers of CYP3A4 together with the two CYPeryF structures that exhibit CB (PDB codes 1EUP and 1EGY) were superimposed, and residues of the CYP3A4 conformers corresponding to the bacterial P450 that are in close contact (less than 5 Å) from the substrates were derived from the structural alignment (Table 1). The C $\alpha$  RMSD of the alignment was 1.47 Å. While the residues of the active and effector sites may change depending on the size, shape, and conformation of the substrates, there is a common core for these sites. The active site consists of the I helix denoted SRS4 and of the BC loop connecting helices B and C denoted SRS1 (see Figure 2). The residues forming the active binding site are I301, F304, A305, G306, and T309 of SRS4 and I118 and S119 of SRS1. The active binding site may include part of the FF' loop, denoted SRS2, as seen in the 1TQN conformer. The R212 residue of SRS2 serves as an active site residue depending on its rotamer orientation. In addition, it may include I369 and A370, a region between the K helix and the  $\beta$ 1 sheet denoted as SRS5. As can

(48) Gotoh, O. *J. Biol. Chem.* **1992**, *267*, 83–90.

(49) McArthur, A. G.; Hegelund, T.; Cox, R. L.; Stegeman, J. J.; Liljeborg, M.; Olsson, U.; Sundberg, P.; Celander, M. C. *J. Mol. Evol.* **2003**, *57*, 200–211.

(50) Peterson, J. A.; Graham-Lorence, S. E. In *Cytochrome P450: Structure, Mechanism and Biochemistry*, 2nd ed.; Ortiz de Montellano, P. R., Ed.; Plenum Press: New York, 1995; pp 151–180.

**Table 1.** Active and Effector Binding Site Residues in CYP3A4 and CYPeryF

active eryF <sup>a</sup>	active 3A4 <sup>b</sup>	effector eryF <sup>a</sup>	effector 3A4 <sup>b</sup>
N89	I118	Y75	F108
V237	I301	F86	M114
A241	A305	L175	F213
G242	G306	V237	I301
A245	T309	L240	F304
P288	A370	A241	A305

<sup>a</sup> Active and effector site residues of CYPeryF obtained from close contacts between substrates and enzyme residues. <sup>b</sup> Corresponding residues of CYP3A4 obtained from a multiple structure alignment with CYPeryF structures.

be seen from Figure 7a, the active binding site interactions with diazepam consist of three hydrogen bonds and a T-shaped  $\pi$ - $\pi$  stacking interaction between F304 and the benzyl moiety of diazepam. In addition there is a  $\pi$ - $\pi$  stacking interaction between the active and effector substrates involving the two aromatic rings of the substrates. The hydrogen bonds are between the carbonyl oxygen of diazepam and the hydroxyl hydrogen of T309 (partial charges  $-0.455$  and  $0.430$ , respectively), a methyl hydrogen of diazepam and the carbonyl oxygen of F304 (partial charges  $0.172$  and  $-0.510$ , respectively), and a benzyl hydrogen of diazepam and the hydroxyl oxygen of S119 (partial charges  $0.118$  and  $-0.660$ , respectively). The effector site common core residues consist of SRS4 and SRS2 (see Figure 2). The residues forming the effector binding site are R212 and F213 of SRS2 and F304, A305, and T309 of SRS4. They may include F108 and M114 of SRS1, I369, A370, and M371 of SRS5, and L482 and L483 of the  $\beta$ 4 sheet denoted SRS6. From the CYPeryF structures and from the simulations performed on CYP3A4, it can be inferred that the conserved I helix (SRS4) which is in close proximity to the active oxygen species is part of an interface between the active and effector binding sites, with F304 and A305 being major residues forming this interface. In contrast to the active binding site interactions that are electrostatic to some extent and involve hydrogen bonding, the interactions of the effector binding site with diazepam are less specific and more hydrophobic and include aromatic ring interactions. The interactions include a T-shaped  $\pi$ - $\pi$  stacking interaction between F213 and the chloride-containing aromatic ring of diazepam and  $\pi$ - $\pi$  stacking interactions between F304 and the benzyl ring of the active substrate with the benzyl ring of the effector substrate (Figure 7b). There are also nonspecific VDW interactions between R212 and L482 and the effector substrate (data not shown).

To understand the influence of the effector on the metabolism of the active diazepam, the distances between the hydrogen atoms of the  $\beta$  carbon that are to be abstracted en route to a hydroxylation reaction and the active oxygen of CpdI were measured in the presence and absence of the effector. A hydroxylation reaction generally occurs by abstraction of a hydrogen atom by the active oxygen species followed by a radical rebound.<sup>2,4</sup> The working hypothesis is that the closer the hydroxylated hydrogens are to the CpdI oxygen, the greater the probability that those hydrogen atoms will be hydroxylated. The active diazepam molecule was docked into a configuration favorable for hydroxylation with the distance between the  $\beta$  carbon hydrogens and CpdI oxygen as close as possible. Without the presence of the effector, in both conformers the hydrogen

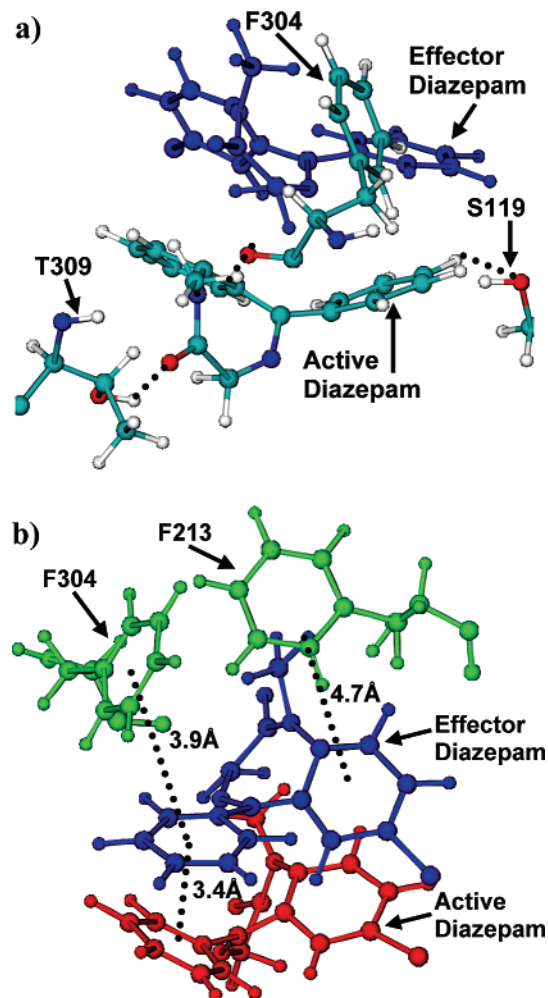


**Figure 7.** Close contacts between the diazepam molecule and the 1W0E conformer at the active and effector binding sites. (a) Active site–diazepam interactions. The effector substrate is colored blue, and the active substrate and enzyme residues are colored by atom. The dotted lines represent hydrogen bonds. (b) Effector site–diazepam interactions. The effector substrate is colored blue, the active one is colored red, and the enzyme residues are colored green. The dotted lines represent minimum distances between aromatic rings.

atoms of the  $\beta$  carbon were found to drift away from the oxygen atom of CpdI, from 2 to 5 Å in 1TQN and up to 8 Å in the 1W0E conformer (Figure 8). *With these distances, it is unlikely that a hydroxylation reaction could proceed.* This observation agrees with experimental results indicating that when the diazepam concentration is low, the percentage of CYP3A4 enzyme in which the two substrates exist in the active site is also low and the yield of hydroxylation product decreases. Addition of the effector dramatically reduced the  $\beta$  carbon hydrogen–oxygen distances in the 1W0E conformer (Figure 8a), whereas in the 1TQN conformer this distance is not affected (Figure 8b).

After 12 ns of simulations, the average distances between the abstracted hydrogen atom and the active oxygen were 3.2 and 4.8 Å in 1W0E\_C and 1TQN\_C, respectively (see the SI). Again we see that the 1W0E conformer agrees with the experimental results: at high levels of diazepam concentration, where the fraction of enzyme bound to two substrates is expected to be higher, the main path of metabolism is hydroxylation. We conclude that CB is simulated in the 1W0E

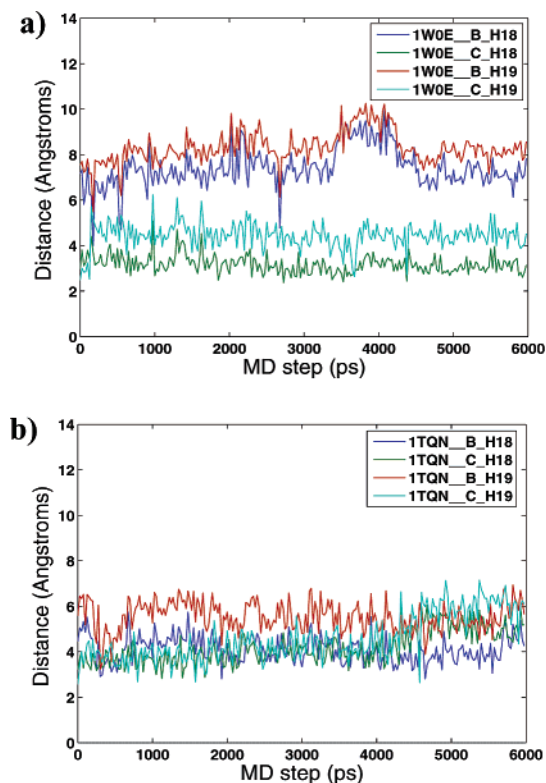


**Figure 8.** Distance between the active oxygen of CpdI and the hydrogens prone to abstraction along the simulations with one and two substrates in both conformers: (a) distance between H18 and H19 (the  $\beta$  carbon hydrogens) and the CpdI oxygen in the 1W0E conformer dynamics with one substrate (1W0E\_B) and two substrates (1W0E\_C); (b) distance between H18 and H19 (the  $\beta$  carbon hydrogens) and the CpdI oxygen in the 1TQN conformer dynamics with one substrate (1TQN\_B) and two substrates (1TQN\_C).

conformer and that the addition of the effector resulted in a preferred conformation of the active diazepam for the hydroxylation reaction. CB was manifested by a low RMSD from the initial structure in the MD simulation of the active and effector diazepam in comparison to the single bound diazepam in 1W0E and in short distances between the hydroxylated hydrogens and the active CpdI oxygen, thereby favoring C–H hydroxylation reactions. In addition to direct interaction with the active diazepam, the effector interacts with the enzyme, and the different ways the effector impacts the CYP3A4 conformers may explain the different results obtained for the conformers and the lack of CB in the 1TQN conformer. As seen in Figure 9, the VDW surface of F304 is larger and more exposed in the 1W0E conformer than in the 1TQN conformer. This results from the extended surface of the effector site, where R212 faces the active site and maintains close contact with F304 in 1TQN. F304 is one of the most flexible residues of the I helix and very close to the heme moiety, thus influencing the active substrate orientation. Stabilization of F304 could lead to a more efficient oxidation, and the lowered accessibility of this residue by strong interaction with R212 prevents the possibility of the effector exerting its influence on the enzyme. Several experimental results support the notion that F304 is a key residue in CB: It was shown that mutating F304 by a larger residue (Trp) resulted in hyperbolic progesterone hydroxylase activity of CYP3A4 without homotropic cooperativity as observed in the unmutated

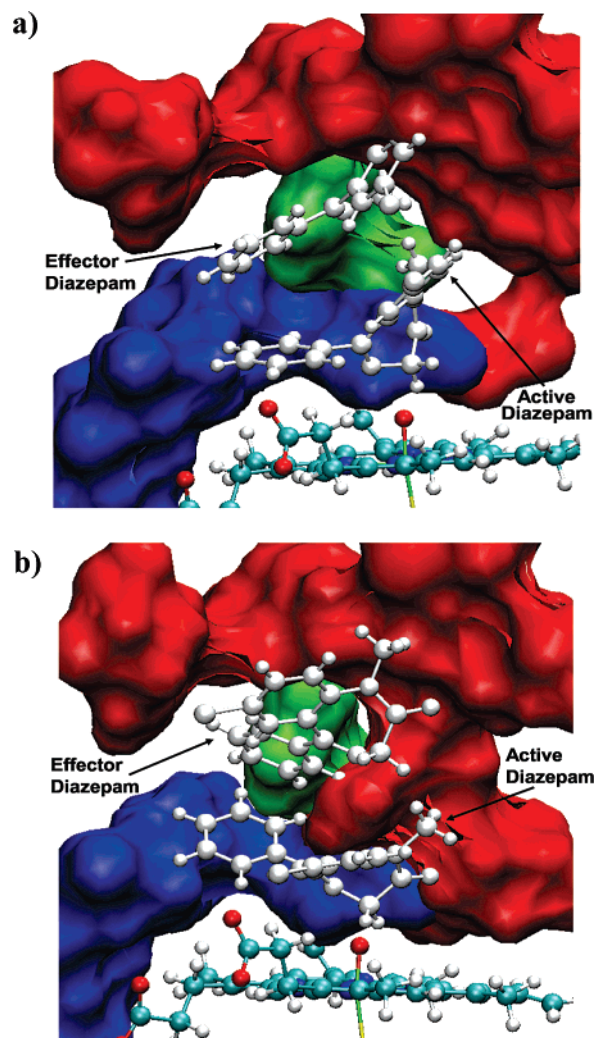


**Figure 9.** VDW surface of the interface between the active and effector surface of binding sites. The active site surface is colored blue, the effector site surface is colored red, and the F304 surface is colored green. The diazepam molecules are represented as CPK models and colored gray. The CpdI moiety is represented as a CPK model and colored by atom. Key: (a) 1W0E conformer; (b) 1TQN conformer.

enzyme.<sup>51</sup> In another study F304 was replaced by a smaller residue (Ala) displaying altered flavenoid stimulation of the hydroxylation of progesterone.<sup>52</sup>

**3.3. Covariance Analysis.** Covariance matrix plots were calculated from the first 3 ns of the simulations of one and two substrates bound to the CYP3A4 conformer using X-PLOR software.<sup>53</sup> The covariance ( $S_{ij}$ ) is defined in eq 1, where  $x(i)$

$$S_{ij} = \frac{\langle x(i) x(j) \rangle}{[\langle x(i)^2 \rangle \langle x(j)^2 \rangle]^{1/2}} \quad (1)$$

and  $x(j)$  are the coordinate displacements relative to the average positions of atoms  $i$  and  $j$ . The covariance analysis was performed to inspect correlated changes in terms of side chain movements within the active and effector sites upon addition

- (51) Domanski, T. L.; He, Y. A.; Harlow, G. R.; Halpert, J. R. *J. Pharmacol. Exp. Ther.* **2000**, *293*, 585–591.  
 (52) Ueng, Y. F.; Kuwabara, T.; Chun, Y. J.; Guengerich, F. P. *Biochemistry* **1997**, *36*, 370–381.  
 (53) Brunger, A. T. *X-PLOR. A system for X-ray crystallography and NMR*, version 3.1; Yale University Press: New Haven, CT, 1992.



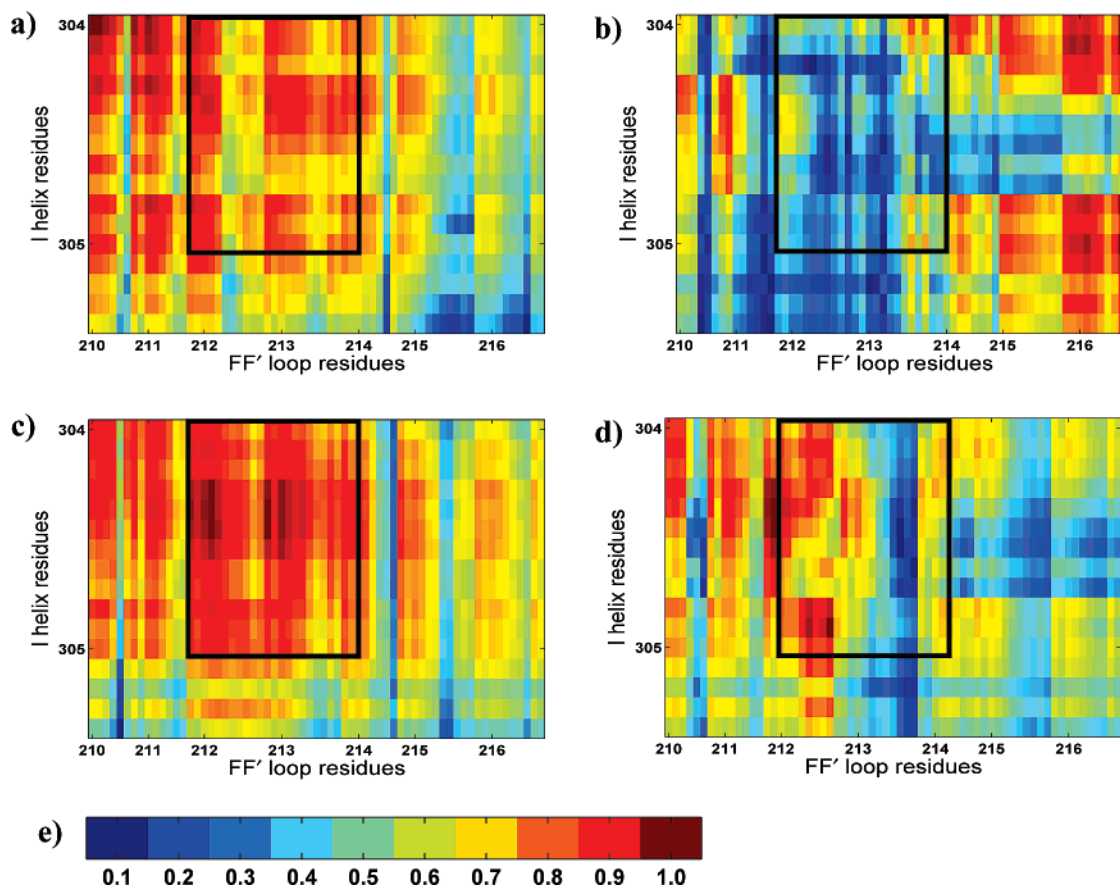


**Figure 10.** Covariance matrix (CM) plots of the spatial displacement between the atoms of residues F304 and A305 and the atoms of the FF' loop residues along the first 3 ns with one and two substrates: (a) 1W0E simulation with one substrate; (b) 1TQN simulation with one substrate; (c) 1W0E dynamics with two substrates; (d) 1TQN dynamics with two substrates; (e) scale of the covariance of the spatial displacement,  $S_{i,j}$ , between atoms  $i$  and  $j$  as calculated according to eq 1.

of the effector substrate. The covariance was calculated between the atoms of residues F304 and A305 and the FF' loop residues to investigate the impact of the effector on the movements of these residues and to obtain insight into the spatial “cross talk” between the core effector site residues (mainly the FF' loop) and the active site residues (mainly F304 and A305). As depicted in Figure 10a,c, when the 1W0E\_B and 1W0E\_C simulations were compared, the covariance between F304 and residues R212 and F213 increased by 2 units of scale (bolded rectangle). This trend was not noticed when 1TQN\_B and 1TQN\_C simulations were compared. There, while the covariance between F304 and R212 increased, the covariance between F304 and F213 remained very low. In the 1W0E conformer dynamics, the addition of the effector diazepam increased the correlation of the movements between the effector site and the active site.

It seems reasonable to conclude that the enhanced movement correlation between F304 and F213 was mediated by the effector since it interacts with both F304 and F213 as seen in the RMSD analysis and in Figure 7b. The effector decreased the RMSD of both residues from the initial structures in the 1W0E\_C simulation and enhanced a stronger interaction between the two phenylalanine residues. To inspect long-range effects induced by the effector molecule, we performed a global all against all C $\alpha$  covariance analysis. We found that the addition of the

effector decreases the covariance of the movement between the 283–293 loop residues (close to the I helix) and several parts of the enzyme including helices D, I, and K, the region between the  $\beta$ 1 sheet and the K' helix, and the BC loop by 4 degrees of scale (see the SI). On the other hand, these parts of the enzyme are correlated to the loop movement in the single-ligand-bound state. This may constitute long-range effects of the effector on the entrance of the access channel (especially in the BC loop and the  $\beta$ 1 sheet) where the effector slightly closes the channel and thereby reduces the chances of entry and competition of other substrates with the active substrate, hence making the oxidation more efficient. However, as this loop is very flexible and as it was modeled computationally, we find these results to be inconclusive. There exists a PDB file containing a CYP3A4 bound to progesterone<sup>27</sup> in which the substrate is placed outside the heme pocket, in close proximity to the FF' loop, and interacting with F213. In another structure of warfarin<sup>54</sup> bound to CYP2C9, the substrate is placed inside the active site but in a far corner not in a position for oxidation. When the two structures were superimposed by their C $\alpha$  atoms, warfarin and progesterone were positioned at both sides of the FF' loop of CYP3A4 and in close proximity to F213 (see the SI). The facts that (a) both progesterone and testosterone share the same steroidal scaffold, (b) site-directed mutagenesis studies show that FF' loop residues are involved in CB of testosterone,<sup>5</sup> (c) a heme remote allosteric site exists,<sup>25</sup> and (d) the proges-

(54) Williams, P. A.; Cosme, J.; Ward, A.; Angove, H. C.; Matak, V. D.; Jhoti, H. *Nature* **2003**, *424*, 464–468.

sterone structure is bound outside the heme pocket all make the FF' loop a putative remote binding site. However, as there is no structural evidence for two substrates, one placed at the progesterone site and another inside the active site, the possibility for a long-range allosteric site is still unclear. Several reports argued about a three-site model for CYP3A4 where three substrates are complexed with the enzyme and are responsible for the atypical kinetics, with at least two binding sites being catalytic.<sup>18,55</sup> It is possible that the region of the FF' loop facing the surface of the enzyme is a third site and that interactions with the loop mediate a closer interaction between F213 and F304 and thereby stabilize F304 as does the effector in our work. We suggest that there may be complementarity between short- and long-range effects. Thus, interactions with F213, stabilizing the active site residues, may play a key role as this residue is exposed to the surface of the protein, faces the active site, and is very flexible, as observed in the CYP3A4 ketoconazole complex. In this structure, the binding of ketoconazole resulted in larger movements of the FF' loop including F213 and revealed the ability of the F213 residue and its surroundings to reorient their positions. Future mutation studies are needed to further reinforce the importance of F304 and F213 residues in cooperative binding.

#### 4. Conclusions

To gain insight into the mechanism of CB in CYP3A4, we investigated the impact of the addition of an effector diazepam molecule on an active oxidized diazepam in the active site of CYP3A4 and on the interactions of the effector with the protein. Our simulations indicated that CB could be observed in only one of the two CYP3A4 conformers (1W0E) due to a difference in the positioning of R212. When R212 faces the active site, it hinders the ability of the effector molecule to exert its effect on the protein. We conclude that the CB mechanism involves interactions between the effector and the active substrate as well as between the effector and the protein and thereby influences

side chain movements. Our results suggest that F304, located at the I helix proximal to the active oxygen species, plays a key role in CB. This residue is bulky and flexible and may hinder the proper active substrate orientation and determine the efficiency of the oxidation reaction. In the CYP3A4 conformer where CB was observed, addition of the effector molecule hampered the flexibility of F304 and of its surroundings (especially F213) and *induced a short distance between the abstracted hydrogen and the active oxygen of CpdI*.

A long-range effect of the effector molecule cannot be ruled out, and we propose F213 as a key residue in long-range effects, possibly caused by interaction between the effector and the FF' loop on the surface of the protein. F213 can also be stabilized inside the active site as occurred in our simulation. Additional mutational and kinetic studies and structural evidence for multiple substrates simultaneously bound to CYP3A4 are needed to further probe these observations and deepen the understanding of the mechanism of CB.

**Acknowledgment.** We thank Dr. K. Gunasekaran for helping with the covariance analysis and Drs. Yongping Pan and Buyong Ma for helpful discussions. This project has been funded in whole or in part with federal funds from the National Cancer Institute, National Institutes of Health, under Contract N01-CO-12400. This research was supported (in part) by the Intramural Research Program of the NIH, National Cancer Institute, Center for Cancer Research. The research at The Hebrew University of Jerusalem (S.S. and C.H.) was supported by the German Federal Ministry of Education and Research (BMBF) within the framework of the German-Israeli Project Cooperation (DIP). This study utilized the high-performance computational capabilities of the Biowulf PC/Linux cluster at the National Institutes of Health, Bethesda, MD (<http://biowulf.nih.gov>).

**Supporting Information Available:** Full author list of refs 40 and 41 and diazepam force field. This material is available free of charge via the Internet at <http://pubs.acs.org>.

JA066007J

(55) Hosea, N. A.; Miller, G. P.; Guengerich, F. P. *Biochemistry* **2000**, *39*, 5929–5939.